

Analog Direct Path Interference Suppression for FM Based Passive Radars

Tamas Peto, Levente Dudas, Rudolf Seller
Budapest University of Technology and Economics
Broadband Infocommunications and Electromagnetic Theory
Remote Sensing Laboratory
Budapest, Hungary
peto@hvt.bme.hu, dudas@hvt.bme.hu, seller@hvt.bme.hu

Abstract—In passive radar systems the direct path interference strongly limits the detection performance, and demands the application of high resolution ADCs (Analog to Digital Converter). In this paper a direct path interference suppression technique is presented which operates in the analog domain prior to the digitalization. Using the introduced interference mitigation procedure the dynamic range required to the received signal can be effectively decreased, allowing the use of low resolution ADCs and low cost general purpose SDR devices. Laboratory measurement results taken with an FM based demonstrator system shows $20dB$ suppression. While in real environment $15dB$ detection performance enhancement could be evinced with field trials.

I. INTRODUCTION

In recent times the passive radar researches are becoming more and more prominent due to they limited hardware resource requirements and the availability of the wide range of IOs (Illuminators of Opportunity). For long range aerial surveillance purposes the most commonly used IOs are the DVB-T (Digital Video Broadcast- Terrestrial), DAB (Digital Audio Broadcast) and the commercial FM (Frequency Modulation) radio broadcast signals [4], [7]. The latest researches and system developments have shown that the DVB-T signal has outstanding parameters in terms of radar surveillance [3], [7]. The main reasons of that is the high transmitter power, the favourable ambiguity function and the reasonable large signal bandwidth that grants a few tens of meter range resolution. At the same time the FM transmitters operate with even higher transmitter power, but with a much smaller signal bandwidth, which strongly limits their efficiency in terms of range resolution. However the FM IOs are not the best candidates, the utilization of the IO diversity can greatly enhance the success of detection and parameter estimation. This mode of operation is discussed by M. Edrich et al. in [5]. In this paper we are focusing on FM based systems in order to develop a low-cost supplementary radar platform next to the more efficient DVB-T based systems.

When it comes to cost optimization, SDRs (Software Defined Radio) are one of the best choices. It is now a common practice to use SDRs on the RF (Radio Frequency) receiving side of the passive radar systems [6], [8]. While most systems use high-end SDR architectures with high resolution ADCs, little attention is being paid to the application of the low cost

commercially available SDRs. The main reason of that, is the insufficient dynamic range that the low resolutions ADCs can handle on these devices. In passive radar applications the RF receiver must be able to ensure the reception of the high power direct path signal and the weak reflected signal simultaneously. The power level difference between these components can exceed $100dB$ [1], [8]. In order not to degrade the received signal purity the dynamic range of the signal must be reduced prior to the digital conversion when low resolution ADCs are applied.

Shentang Li et al. in [2] have proposed an analog filter loop that is able to suppress the high power direct path signal before the digitalization step. In their work the control loop is implemented fully in the analog domain using a VCA (voltage controlled attenuator), a VCPS (Voltage Controlled Phase Shifter) and amplitude discriminators. Using this technique they could achieve $35dB$ attenuation in real environment. In this paper their analog DPIS (Direct Path Interference Suppression) technique is further developed in a way to achieve a more compact IQ modulator based design and a more advanced control loop implemented in the digital domain. The development is carried out using low cost commercially available SDRs having 8 bit ADC resolution.

In the next section the effects of the direct path interference on the target detection is discussed. The third section introduces into the theory of the the analog DPIS cancellation. The fourth section presents the system architecture of the used demonstrator hardware. In the last sections the operation of the system is verified with laboratory and field measurements.

II. THEORY OF THE DETECTION PERFORMANCE DEGRADATION

Figure 1 illustrates the considered propagation scenario. In a general case the signal received by a passive radar receiver is composed of the direct path signal, the target reflection, clutter and the receiver noise.

Let us assume that we use two independent receiver channels on the passive radar receiver side. These are the reference and the surveillance channels. The received signal on the

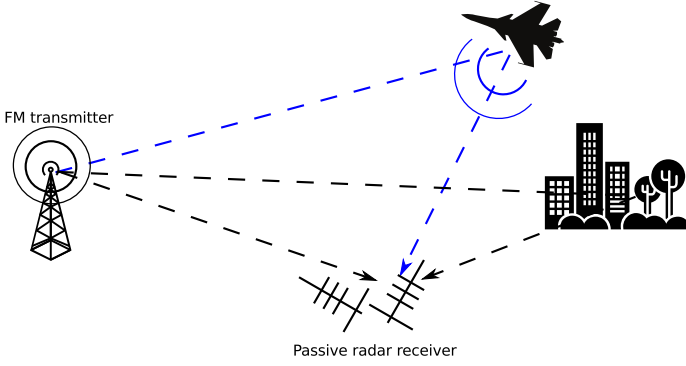


Fig. 1: Passive radar signal modell

reference channel can be formulated as follows:

$$x_r(t) = \sum_{m=0}^{M-1} h_r[m]s(t - \tau_m) + \nu(t), \quad (1)$$

where $s(t)$ denotes the transmitted illuminator signal, $h_r[m] \in \mathbb{C}, m = 0 \dots M-1$ are the propagation factors of the dominant static reflection paths of the reference channel and $\nu(t) \sim \mathcal{N}(0, \sigma_r)$ is the receiver noise, having zero mean and σ_r variance. Note that in practical cases we can fairly guarantee that $h_r[m] = 0$ for non zero time delays $\tau_m \neq 0$ using a highly directional antenna. Namely we receive the direct path only. Beside this on the surveillance channel we receive also the desired target reflection component.

$$x_s(t) = \sum_{k=0}^{K-1} h_s[k]s(t - \tau_k) + \gamma s(t - \tau_t)e^{j2\pi f_D t} + \xi(t), \quad (2)$$

where $h_s[k] \in \mathbb{C}, k = 0 \dots K-1$ are the propagation factors of the dominant static reflection components (clutter) appearing on the surveillance channel and $\xi(t) \sim \mathcal{N}(0, \sigma_s)$ is the receiver noise on the surveillance channel. The reflected signal is described by the $\gamma \in \mathbb{C}$ propagation factor, the τ_t time delay and the f_D Doppler shift parameters. In most cases the surveillance antenna has a much wider beamwidth than the reference antenna in order to cover the full surveillance area. In a conclusion the non zero time delayed clutter components on the surveillance channel are not negligible $h_s[k] \neq 0, \forall k = 0 \dots K-1$.

The amplitude of the propagation factors corresponding to direct path and the reflection path can also be calculated using (3), (4) and (5)

$$|h_r[0]| = \frac{\lambda}{4\pi L} \quad (3)$$

$$|h_s[0]| = \frac{\lambda}{4\pi L} \quad (4)$$

$$|\gamma| = \sqrt{\frac{\sigma \lambda^2}{(4\pi)^3 R_t^2 R_r^2}} \quad (5)$$

In formulas above λ corresponds to the wavelength of the illuminator signal, L denotes the transmitter to receiver distance,

R_t is the transmitter to target distance and R_r is the target to receiver distance. σ denotes the radar cross section of the hypothetical target. Note that, we ignore the antenna gain both on the transmitter and the receiver side. The receiver noise on both channel can be calculated assuming thermal noise only using (6)

$$P_n^{(t)} = \sigma_r^2 = \sigma_s^2 = kTB, \quad (6)$$

where k is the Boltzmann constant, T is the system temperature and B is the illuminator signal bandwidth.

After digitalization the surveillance signal has the following form, where f_s denotes the sampling frequency and n is the discrete time index.

$$x_s[n] = \sum_{k=0}^{K-1} h_s[k]s \left[n - \frac{\tau_k}{f_s} \right] + \gamma s \left[n - \frac{\tau_t}{f_s} \right] e^{j2\pi f_D n} + \xi[n] + q[n] \quad (7)$$

The received signal at this stage is corrupted by the quantization noise described with $q[n]$. For sinusoidal input, assuming full scale ADC drive the power of the quantization noise can be expressed by (8)

$$P_n^{(q)} = P_0 \left(\frac{2\sqrt{2}}{2^U \sqrt{12}} \right)^2, \quad (8)$$

where U is the bit depth of the ADC, and P_0 is the power of the sinusoidal signal. The sinusoidal input drive is an acceptable consideration for FM based IOs according to (12).

After digitalization, in the detection stage the reference $x_r[n]$ and surveillance $x_s[n]$ channels are cross-correlated realizing the matched filtering.

$$\chi[l, f_D] = \sum_{n=0}^{N-1} x_s[n]x_r[n-l]^* e^{-j2\pi f_D n}, \quad (9)$$

where N denotes the number of samples used for the coherent integration. The SINR (Signal-to-Noise plus Interference

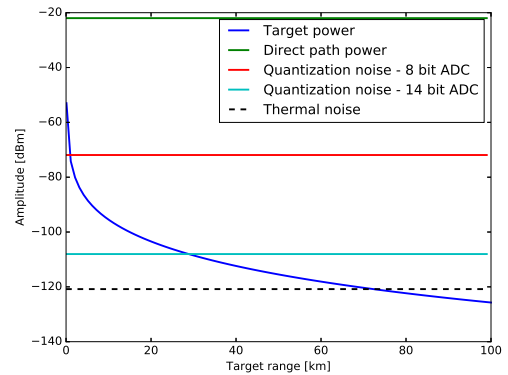


Fig. 2: Power level relations of the surveillance signal components

Ratio) at the output of the cross-correlation detector depends on the purity of the input signals, namely the SINRs of the surveillance and reference channels. In case the reference signal has high enough SINR, the SINR of the target reflection on the surveillance channel can be increased by $\sim N$ using the cross-correlation detector [9]. However, in order to maximize the detection performance the SINR of the surveillance signal should not be degraded even before the detector. Assuming that $P_s = \mathbf{E}\{|s(t)|^2\}$ is the power of the illuminator the SINR of the surveillance channel is written as

$$SINR_{surv} = \frac{P_s |\gamma|^2}{P_s \sum_{k=0}^{K-1} |h_s[k]|^2 + P_n^{(t)} + P_n^{(q)}} \quad (10)$$

Then we can take the following considerations. In a given scenario the direct path signal has the most dominant power $|h_s[0]|^2 \gg \sum_{k=1}^{K-1} |h_s[k]|^2$, $|h_s[0]|^2 \gg P_n^{(t)}$, $|h_s[0]|^2 \gg |\gamma|^2$. Consequently the power level of the direct path signal determines the full scale drive level of the ADC, thus $P_0 = P_s |h_s[0]|^2$.

$$SINR_{surv} < \frac{P_s |\gamma|^2}{P_s |h_s[0]|^2 \left(1 + \left(\frac{2\sqrt{2}}{2^U \sqrt{12}}\right)^2\right)} \quad (11)$$

For better appreciation Figure 2 illustrates the power level relations of a typical scenario. In this particular calculation the baseline distance $L = 30km$, the transmitter power $P_s = 100kW$, the simulation frequency is $f = 100MHz$ and the assumed target radar cross section $\sigma = 100m^2$. Knowing the direct path signal can be filtered very effectively in the digital domain [9], it can be observed that how the quantization noise dominates the surveillance signal and thus decrease its SINR.

III. PRINCIPLES OF THE ANALOG DPIS TECHNIQUE

In this section we develop a signal model to describe the operation of the digitally controlled analog filter circuit. The FM signal transmitted by the used IO is described by (12)

$$s_{FM}(t) = u_c \exp\left(j(2\pi f_c t + 2\pi k_{FM} \int_0^t s_m(\tau) d\tau)\right), \quad (12)$$

where u_c is the amplitude of the carrier signal, f_c is the carrier frequency and $s_m(t)$ is the modulating signal. The frequency deviation is defined as $f_D = k_{FM} \max\{s_m(t)\}$.

Using Carson's formula the relative bandwidth of the FM illuminator signal can be written as:

$$b = 2(f_D + \max\{f_m\})/f_c \quad (13)$$

In practical scenarios the FM illuminators are operating in the VHF (Very High Frequency) band (87.5 – 108MHz) with $f_D = 75kHz$ frequency deviation. According to (13) the relative bandwidth of the signal is small, thus we can approximate the time delay operation with phase shifting. Based on this assumption the direct path interference on the surveillance channel can be mitigated by subtracting the properly scaled reference channel signal from the surveillance

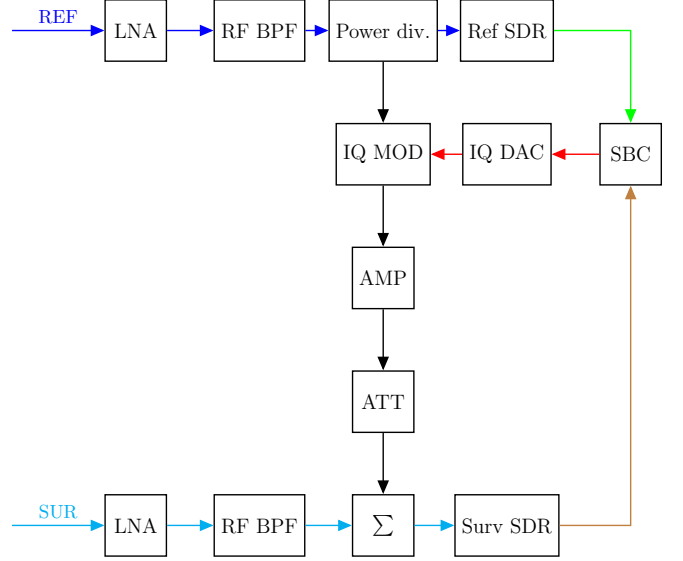


Fig. 3: Block scheme of the SDR based analog DPIS implementation

channel. The filtered analog surveillance channel signal is then written as

$$x_f(t) = x_s(t) - \alpha e^{j\phi} x_r(t) \quad (14)$$

In the following sections we are focusing on the efficient implementation of (14) and on the problem of finding the proper α and ϕ values.

IV. ARCHITECTURE AND CONTROL OF THE PROPOSED ANALOG FILTER

While the scaling and phase shifting is implemented with a VCA and a VCPS in [2], we used an IQ modulator based design to implement the same operation. The block schematic of the proposed system architecture is illustrated in Figure 3.

The signals of the reference and the surveillance channels are first amplified by LNAs (Low Noise Amplifier) to ensure low overall noise figure for the system. In the second stage, the signals are filtered with RF band pass filters. After filtering

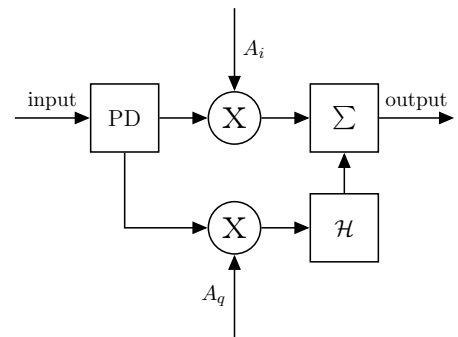


Fig. 4: Block scheme of the IQ modulator

the reference signal, it is divided by a power divider to the cancellation path and to signal path used for the reference channel digitalization. While the reference channel is received and digitalized by the reference SDR the signal on the cancellation path is scaled and phase shifted by an IQ modulator. The block scheme of the modulator is depicted in Figure 4, in which \mathcal{H} denotes the Hilbert transform. The A_i and A_q control voltages for the modulator are produced with two DACs (Digital to Analog Converter) which are programmed from the SBC (Single Board Computer). After IQ modulation the modified reference signal is combined with the received surveillance channel signal in a power combiner. According to the described operation the filtered surveillance channel signal can be written as:

$$x_f(t) = x_s(t) - (x_r(t)A_i + x_r(t)A_q e^{j\frac{\pi}{2}}) \quad (15)$$

Our ultimate goal is to set the proper A_i and A_q values such that the clutter power on the surveillance channel is minimized.

$$\underset{A_i, A_q}{\operatorname{argmin}} \{P_c\}, \quad (16)$$

where

$$P_c = \sum_{k=0}^{K-1} |h_s[k]|^2 \quad (17)$$

is the clutter power. In ideal case the control values are set according to (18).

$$A_i = \Re \{h_k\}, \quad A_q = \Im \{h_k\}, \quad \tau_k = 0 \quad (18)$$

That is the direct path signal is suppressed. Note that the cancellation of a signal component that has larger time delay than the maximum coherent interval $\tau_k > \tau_c$ is not possible due to the phase shifter based system architecture.

To find the optimal A_i and A_q voltages in a sense of (16) the SBC runs an optimization algorithm that continuously download samples from the SDRs and evaluates the cost of the cancellation performance. To obtain the cost of the current control settings, the empirical clutter power is obtained by calculating (19) at every download iteration.

$$\hat{P}_c^{(i)} = \sum_{n=0}^{N-1} x_f[n]x_f[n]^*, \quad (19)$$

where $x_f[n], n = 0 \dots N-1$ are the digitalized samples of the surveillance channel signal $x_f(t)$, and N is the number of processed samples. Here we assumed that the power of the reflected signal is much smaller than the clutter power, thus

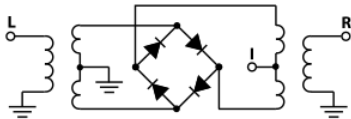


Fig. 5: Schematic of the double balanced mixer used in the IQ modulator

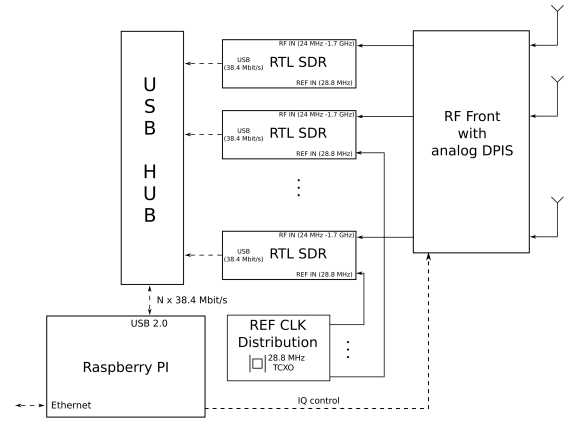


Fig. 6: Block scheme of the SDR based FM passive radar

the contribution of the reflected signal to the overall signal power is negligible $\frac{|r|^2}{P_c} \approx 0$. Note that a metric that calculates the cross-correlation between the reference and the filtered surveillance channels would eliminate the influence of the reflected signal, but the instantaneous estimate of the filtered surveillance channel power does not require the knowledge of the reference signal in any sense.

In the final stage of the algorithm the gain of the receiver should be increased to achieve full scale drive on the ADC and thus realize the SINR improvement on the surveillance channel.

V. MEASUREMENTS

The performance of the analog DPIS method is tested both with laboratory and in-situ measurements. Figure 6 shows the developed FM based passive radar demonstrator system that use low-cost SDRs in conjunction with the previously presented technique. The power divider and power combiner circuits are realized using lumped element Wilkinson networks. The IQ modulator consist of two SRA-1+ double balanced ring mixer to realize the four quadrant multiplication. Its schematic is depicted in Figure 5. The Hilbert transformation is realized using an LC phase shifter. Note that there is no need to realize high performance Hilbert transformation, as the unity amplitude transfer and phase shift errors are inherently corrected by the IQ tuning algorithm. The amplification at the output of the IQ modulator stage is tuned in a way to maximize the allowable direct path power level difference at the input of the RF-front unit ($\frac{|h_r[0]|^2}{|h_s[0]|^2}$). Signals at the output is received by the Realtek RTL2832U and R820T chipset based SDRs. The digitalized samples are then forwarded to a Raspberry Pi which then process the recorded samples and tune the A_i and A_q values using an optimizer algorithm.

A. Cancellation performance

The operation of the described suppression method is tested in laboratory environment using an FM test transmitter. The FM test signal is splited by a power divider and connected directly to the two input of the RF-front unit. A differential evolution algorithm is utilized to tune the control voltages

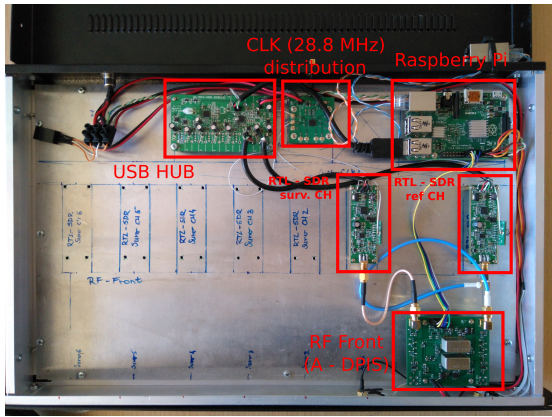


Fig. 7: Experimental dual channel coherent receiver with the RF front module implementing the A-DPIS method

depending on the estimated surveillance channel power. Figure 8 shows the spectrum of the surveillance channel before and after running the tuning algorithm. As it can be seen approximately 20dB suppression is achieved. The blue curve shows the original signal spectrum, while the green curve represents the spectrum obtained after the tuning process. Finally the red curve shows the spectrum, after the gain of the internal IF (Intermediate Frequency) amplifier has been increased in the SDR of the surveillance channel. Let us emphasize that the noise floor has also raised, meaning that the thermal noise floor is now dominating the receiver noise instead of the quantization noise.

B. Field measurements

In order to validate the operation of the proposed direct path suppression technique in real environment field measurement has been taken near to the Liszt Ferenc International Airport in Hungary. During the measurement landing airplanes have been observed. Using this scenario a well controlled measurement could be created. The detected targets had almost the same

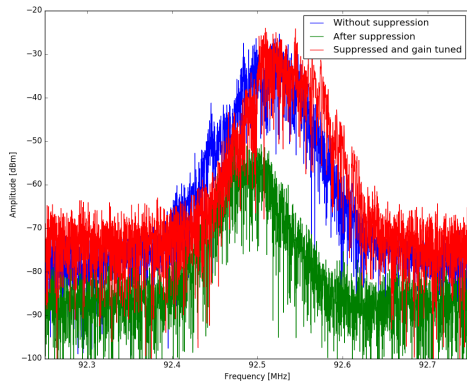


Fig. 8: Measured spectrum of the filtered and original surveillance channel in laboratory environment

trajectory that greatly facilitated the correct evaluation of the results.



Fig. 9: Setup of the in-situ measurement

Figure 9 shows the picture of the installed measurement setup. The two VHF band Yagi antennas are used for the A-DPIS experiment, while the UHF band antennas are used for a DVB-T based control system. The antenna on the left is used as the reference antenna, which was pointed to an FM radio station located at the Széchenyi-hill. In contrast, the surveillance antenna was directed in the direction of the approaching airplanes. The experimental measurement was taken at 89.5 MHz , using an IO having 77 kW transmitter power.

In order to evaluate the performance of the proposed technique two measurement set has been recorded. Measurements in the first set are made without using A-DPIS, while the second set contains measurement with using A-DPIS. The tuning of the A_i and A_q control values are conducted in two stages. In the first stage the cost function has been scanned on a coarse grid. After the approximate of the best values have been found on this grid, a gradient optimization algorithm is initialized and the more precise control voltages are obtained

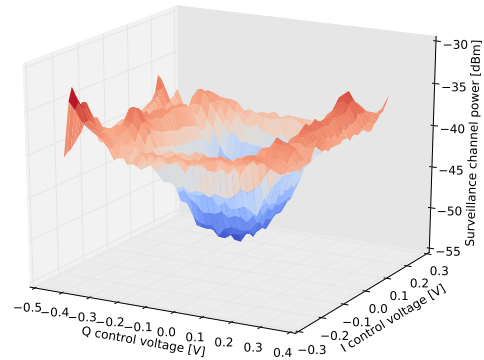


Fig. 10: Cost function of the A-DPIS optimizer

and configured. Once the surveillance channel power has been decreased the IF amplifier gain of the receiver is increased to lower the influence of the quantization noise. In Figure 10 the evaluated cost function used by the optimizer is shown. The quadratic shape of the function can be clearly observed.

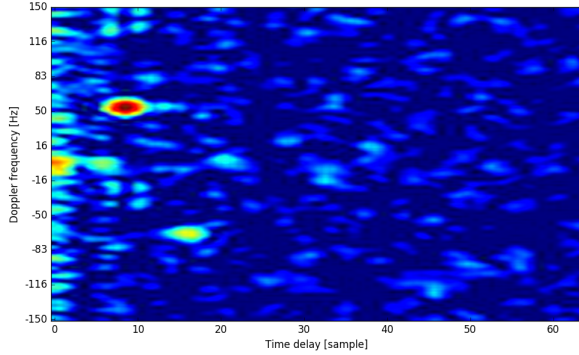


Fig. 11: Landing airplanes on the range-Doppler map. (1 sample delay corresponds to 1500 m)

Figure 11 shows the obtained range-Doppler map when the A-DPIS method is applied. The correlation peak having positive Doppler frequency corresponds to the target reflection of a currently landing airplane, while the one having negative Doppler frequency corresponds to an airplane approaching to runway. After recording the surveillance data from several landing airplanes in both measurement set, the detected targets are identified on the range-Doppler maps and the correlation peaks corresponding to the target reflection are extracted. Then the metric described by (20) have been evaluated for all detection associated to the landing airplanes.

$$M[v] = \frac{|\chi[l, f_D]|^{2(v)}}{P_{surv}^{(v)}}, \quad (20)$$

where v is the index of the measurement and $P_{surv}^{(v)}$ is the average power of the surveillance signal calculated for the v th snapshot. As the range resolution is quite poor, several detections have been made on a given target in the same range cell. From above the available metric values the median has been selected for each range cell. The final results are presented in Figure 12. The improvement arising from the application of the A-DPIS method is clearly visible.

VI. CONCLUSION AND PERSPECTIVES

This paper addresses a DPIS method implemented in the analog domain prior to the digital conversion. Using the designed hardware architecture and the described technique, the reception of the passive radar signals becomes feasible on SDRs which applies low resolution ADCs. As the implementation of the presented technique is not straightforward for signals that have large relative bandwidth further researches may focus on this problem. Beside this, the multichannel operation is necessary to measure the direction-of-arrival of the reflected signal to calculate the exact Cartesian coordinates

of the detected target. In order to realize such an operation the suppression must be performed on spatially coherent receiver channels. The analysis of the development of the optimal IQ control values over time also designate a promising research direction.

ACKNOWLEDGMENT

The work was created in commission of the National University of Public Service under the priority project KÖFOP-2.1.2-VEKOP-15-2016-00001 titled „Public Service Development Establishing Good Governance” in the Bay Zoltán Ludovika Workshop.

REFERENCES

- [1] H.D. Griffiths and C.J. Baker, *Passive coherent location radar systems. Part 1: Performance prediction*, IEE Proceedings - Radar, Sonar and Navigation, **152**,(3), pp 153-159, 2005
- [2] Shentang Li, Zhigang Wang, Hong Wan, *The Analysis and Design of Direct Path Interference Cancellation in FM Radio-Based Passive Radar*, 2006 CIE International Conference on Radar, Shanghai, China, 16-19, Oct, 2016
- [3] M. Radmard, M. Bastani, F. Behnia, M. M. Nayebi, *Cross ambiguity function analysis of the '8k-mode' DVB-T for passive radar application*, International Radar Symposium (IRS 2010), Vilnius, Lithuania, 16-18 June 2010
- [4] M. Malanowski, K. Kulpa et al., *Experimental results of the PaRaDe passive radar field trials*, International Radar Symposium (IRS 2012), Wawsaw, Poland, 23-25 May 2012
- [5] M. Edrich, A. Schroeder, V. Winkler, *Design and performance evaluation of a FM / DAB / DVB-T multi-illuminator passive radar system*, IET International Conference on Radar, Glasgow, UK, 22-25 May 2012
- [6] A. Capria, D. Petri, C. Moscardini et al., *Software-defined Multiband Array Passive Radar (SMARP) demonstrator: A test and evaluation perspective*, OCEANS, Genova, 18-21 May 2015
- [7] Tamas Peto, Rudolf Seller, *Quad channel DVB-T based passive radar*, International Radar Symposium (IRS 2016), Krakow, Poland, 10-12 May 2016
- [8] Tamas Peto and Rudolf Seller, *Quad channel software defined receiver for passive radar application*, Archives of Electrical Engineering, **66**,(1), pp 5-16, 2017
- [9] Tamas Peto and Rudolf Seller, *Topics in Radar Signal Processing: Adaptive Clutter Cancellation Techniques for Passive Radars* InTech, ISBN: 978-953-51-5836-3

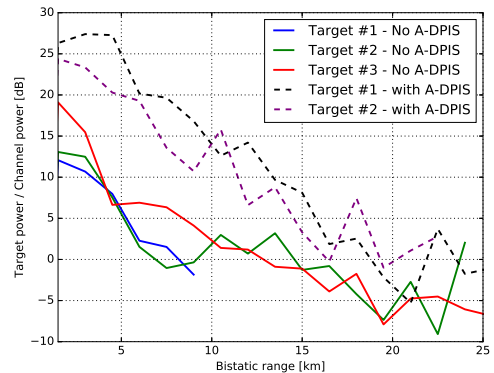


Fig. 12: Performance improvement of the Analog-Direct Path Interference Suppression